

# Application of ICA in Removing Artefacts from the ECG

Taigang He, Gari Clifford and Lionel Tarassenko  
Signal Processing & Neural Networks Research Group  
Department of Engineering Science  
University of Oxford, Oxford, UK

*Routinely recorded electrocardiograms (ECGs) are often corrupted by different types of artefacts and many efforts have been made to enhance their quality by reducing the noise or artefacts. This paper addresses the problem of removing noise and artefacts from ECGs using Independent Component Analysis (ICA). An ICA algorithm is tested on 3-channel ECG recordings taken from human subjects, mostly in the Coronary Care Unit (CCU). Results are presented that show that ICA can detect and remove a variety of noise and artefact sources in these ECGs. One difficulty with the application of ICA is the determination of the order of the independent components. A new technique based on simple statistical parameters is proposed to solve this problem in this application. The developed technique is successfully applied to the ECG data and offers potential for online processing of ECG using ICA.*

**Keywords:** Independent component analysis; artefacts, noise removal; ECG; permutation

## 1. Introduction

In routinely recorded ECGs, many types of noise and artefact are present. Noise is defined to be part of the real signal that confuses analysis (e.g. muscle movements) and artefact is defined to be any distortion of the signal caused by the recording process, such as electrode movement. Many attempts have been made to detect and eliminate noise sources and artefacts from the actual electrocardiographic signals.

Analogue or digital filters are widely used to reduce the influence of interference superimposed on the ECG. Early work on noise and artefact reduction in the ECG used either temporal or spatial averaging techniques [1]. The temporal averaging method requires a large number of time frames for effective noise reduction, while the main drawback of spatial averaging is the physical limitation of placing a large number of electrodes in the same region. Besides linear noise filtering, several adaptive filtering methods have been proposed for separation and identification of the component waves from noisy ECGs [2, 3, 4]. The quasi periodic pattern of the cardiac signal has also been exploited [5, 6, 7] by synchronizing the parameters of the filter with the period of the signal. Other proposed methods include subspace rotations [8], neural networks [9], and bi-spectral analysis [10].

However, many of these methods to filter out the noise and artefacts from ECG are only partially successful. On the one hand, the filters often lead to a reduction in the amplitudes of the component waves, the Q-, R- and S- waves or the QRS complex

[Fig. 1]. On the other hand, some of the noise and artefacts are random in nature and have a wide range of frequency content. Hence the filters fail to remove the interference when it is within the same frequency range as the cardiac signal.

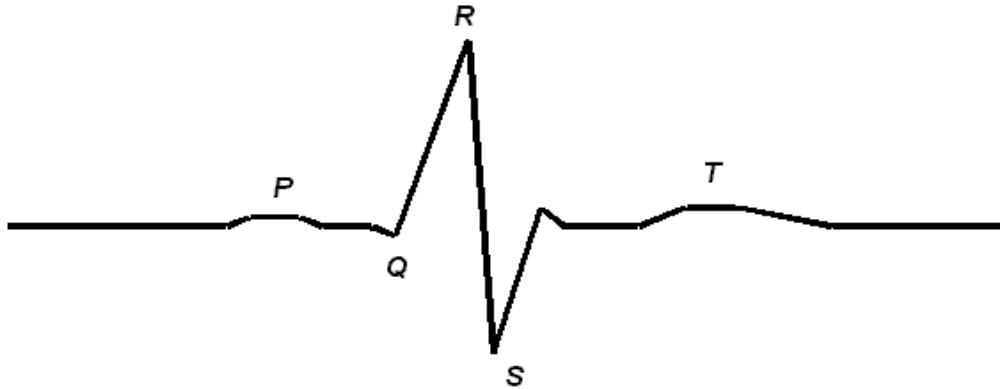


**Fig.1.** Typical ECG waveform with the P, Q, R, S and T waves for one heart beat.

ICA is a newly developed source separation method, and its application to biomedical signals is rapidly expanding [11]. In the field of ECG analysis, Cardoso [12] presented a good example of ICA decomposition for fetal and maternal ECGs recorded simultaneously from 8 electrodes placed on the mother's chest and abdomen. Wisbeck et al. [13] used ICA to isolate the breathing artefacts (large baseline shifts due to the physical movement of the electrodes in relation to the heart) from 8-channel ECG recordings. This showed that the ICA technique was able to enhance the quality of the cardiac signals. However, the breathing artefacts were found in several independent components. Barros et al. [14] proposed a two-layer neural network application of ICA to eliminate artefacts from the ECG. In this case, only simulations were carried out to demonstrate the performance of the algorithm. In a recent study, Tong and his colleagues [15] also attempted to remove ECG interference from EEG recordings in small animals using ICA.

Although a comprehensive study on the application of ICA to EEG noise and artefact removal has been carried out by Jung et al. [16], there is still no general approach to ECG noise and artefact removal using ICA. Secondly, it is usually the case that only a few electrodes are used in the clinical environment for the continuous recording of the ECG (12-lead ECGs are in general only recorded for short periods of time, usually a few seconds, when a detailed investigation of the heart condition is required, for example during a drug trial or following a heart attack). Thirdly, there is no ordering of the ICA components (the ICA permutation problem) as with Principal Component Analysis (PCA) [17]. Thus one has to rely on visual inspection for further processing, which is not desirable in routine clinical ECG analysis.

The purpose of this paper is thus threefold. Firstly, it aims to see if ICA can remove noise and artefacts where simple filters fail to do so. The focus is not on a particular type of noise or artefact, hence a more general analysis than previously attempted is described. Secondly, ICA is applied to 3-channel human ECGs recorded from hospital patients in CCU to investigate how ICA performs with a limited number of observations. Thirdly, a technique based on linear statistics is proposed to solve the ICA permutation problem in this application.

The paper begins by describing briefly the ICA model in section 2.1.1 and the algorithm used in section 2.1.2. The technique to solve ICA permutation is proposed in section 2.2. The type of data to be analysed is described in section 2.3. The choice of thresholds for detection of continuous noise and abrupt changes is considered in section 3. Results are then presented in sections 4 together with a discussion and pointers to future work in the last section.

## 2. Materials and methods

### 2.1 Independent component analysis

#### 2.1.1 The basic model

The basic ICA approach uses the following linear model:

$$X = AS \quad (1)$$

where the vector  $S$  represents  $m$  independent sources, the matrix  $A$  represents the linear mixing of the sources, and the vector  $X$  is composed of  $m$  observed signals. Note that no noise term is included in this model, since the estimation of the noise-free model is difficult enough in itself.

A source here means an original signal, i.e. an independent component, like a speaker in the ‘cocktail party problem’[17]. Broadly speaking, the idea of ICA is to recover the original sources by assuming that they are statistically independent. The independence assumption means that the joint *probability density function* (pdf) is the product of the densities for all sources:

$$P(S) = \prod p(s_i) \quad (2)$$

where  $p(s_i)$  is the pdf of source  $i$  and  $P(S)$  is the joint density function.

Denoting the output vector by  $V$ , the aim of ICA algorithms is to find a matrix  $U$  to undo the mixing effect. That is, the output will be given by

$$V = UX \quad (3)$$

where  $V$  is an estimate of the sources. The sources can be exactly recovered if  $U$  is the inverse of  $A$  up to a permutation and scale change.

#### 2.1.2 The algorithms

The estimation of the data model of ICA is usually performed by formulating an objective function, e.g. mutual information or negentropy, and then minimizing or sometimes maximizing it. This transforms the ICA problem to a numerical optimization problem [17].

In this approach, we use the JADE (Joint Approximate Diagonalization of Eigen-

matrices) algorithm developed by Cardoso [18]. The JADE algorithm, which is based on the joint diagonalization of cumulant matrices, has been successfully applied to the processing of real data sets, such as mobile telephone, radar as well as biomedical signals. It is very efficient for separation when there is a small number of observations. Hence, this algorithm is suitable for our approach.

The JADE algorithm can be summarized as follows:

- 1) *Initialization.* Estimate whitening  $W$  and set  $Z=WX$ .

The covariance matrix is defined as  $R_x=E(XX^T)$ , where  $E$  is the mathematical expectation function. Denoting  $D$  as the diagonal matrix of its eigenvalues and  $H$  as the corresponding eigenvectors, a whitening matrix is

$$W=HD^{(-1/2)}H^T \quad (4)$$

- 2) *Form statistics.* Estimate a maximal set  $\{Q_z\}$  of the cumulant matrix.

Given a  $n \times 1$  random vector  $z$  and any  $n \times n$  matrix  $M$ , the cumulant matrix is

$$Q_z(M)=E\{(z^T M z)zz^T\}-R_z tr(MR_z)-R_z M_z - R_z M^T R_z, \quad (5)$$

where  $tr()$  denotes the trace of a matrix.

- 3) *Optimize orthogonal contrast.* Find the rotation matrix  $U$  such that the cumulant matrix is as diagonal as possible. See [18] for details.

- 4) *Separate.* Estimate  $A$  as  $V=UW^{-1}$  and the source as  $V=U^{-1}X$ .

In our problem, the rows of the input matrix  $X$  are the three ECG signals. The reconstructed ECG can be derived from  $X'=UV'$ , where  $V'$  is the matrix of derived independent components with the row representing the noise or artefacts set to zero. Suppose the second ICA component represents noise.  $V'$  can then be written as

$$V=\begin{bmatrix} V_{11} & V_{12} & \cdots & V_{1N} \\ 0 & 0 & \cdots & 0 \\ V_{31} & V_{32} & \cdots & V_{3N} \end{bmatrix} \quad (6)$$

where  $V_{ij}$  ( $i=1, \dots, 3$ ,  $j=1, \dots, N$ ) are the elements of matrix  $V$ , and  $N$  represents sample number.

All studies reported in this paper were carried out using the JADE algorithm implemented in MATLAB 5 (See <http://tsi.enst.fr/icacentral/algos.html>).

## 2.2 Identification of noise and artefact component

From the ICA model in Eq. (1), it can be seen that one cannot determine the order of the independent components, as a permutation matrix  $P$  and its inverse  $P^{-1}$  can be added in the model to give  $X=AP^{-1}PS$ . The elements of  $PS$  are the original independent variables, but in a different order. The matrix  $AP^{-1}$  is therefore a new unknown mixing matrix, to be solved by the ICA algorithms. Furthermore, the order of components may also vary from one data segment to the next.

Therefore one has to rely on visual inspection of the ICA components for further processing, a requirement which is not desirable in routine clinical ECG monitoring. In practice, the separated components tend to have more distinctive properties than the original signals both in time and frequency domains. Hence we may employ the statistical properties of these waveforms and recognize them automatically.

### 2.2.1 ECG, continuous noise and abrupt changes

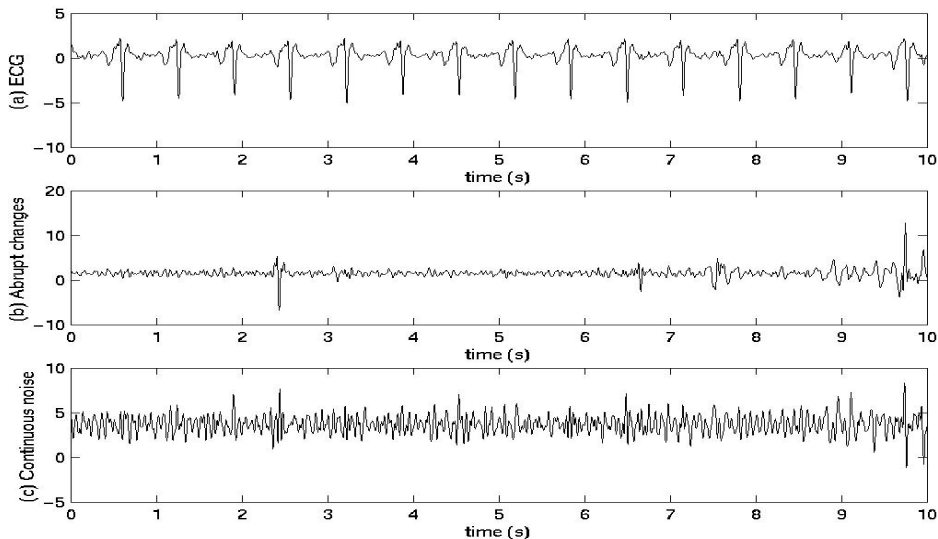


**Fig. 2.** Typical waveforms of (a) the ECG, (b) abrupt changes and (c) continuous noise

According to their morphology in the time domain, the ICA components of ECG recordings can be roughly divided into three categories: normal ECG, continuous noise and abrupt change. As an illustration, consider the waveforms in Fig. 2.

The data has a length of 10 seconds. It can be seen that each has visually distinct characteristics. It is therefore likely that there exist proper indices to distinguish the continuous noise and abrupt changes from normal ECGs.

The identifying procedure will be composed of two main steps: identifying noise using kurtosis and detecting abrupt changes using variance.

## 2.2.2 Kurtosis

The kurtosis is the fourth-order cumulant. For a signal  $x$ , it is classically defined as

$$Kurt(x) = E(x^4) - 3[E(x^2)]^2 \quad (7)$$

The kurtosis is zero for Gaussian densities. For continuous noise as shown in Fig 2(c), the Kurtosis value is much smaller compared with that of normal ECG (Fig. 2(a)). In our approach, a threshold is chosen from analysis of sample waveforms, and a component whose modulus of kurtosis is below this threshold will be considered as continuous noise.

The main reason for choosing kurtosis is its simplicity. Computationally, kurtosis can be estimated by using the fourth moment of the sample data. However, kurtosis also has some drawbacks in practice. The main problem is that kurtosis can be very sensitive to outliers [19] or abrupt changes. Its value may depend on only a few observations in the tails of the distribution, which may be erroneous or irrelevant observations. Abrupt changes cannot be differentiated from normal ECG by using kurtosis, hence another index is needed for this task.

## 2.2.3 Variance index

For a signal  $x(n)$  with  $N$  samples, the variance is known as:

$$Var_x = \sum_{n=1}^{N-1} [x(n) - \bar{x}(n)]^2 \quad (8)$$

where  $\bar{x}(n)$  is the mean value of  $x(n)$ .

The problem is that one cannot determine the variances (energies) of the independent components. In Eq. (1), since both  $A$  and  $S$  are unknown, any scalar multiplier in one of the sources could always be cancelled by dividing the corresponding column of the mixing matrix  $A$  by the same scalar. Therefore, ICA algorithms usually assume that each component has unit variance. The matrix  $A$  is then adapted in the ICA solution methods to take this restriction into account.

The abrupt changes are usually short transients, as is shown in Fig. 2(b). There are several ways which could be used to detect these changes. Most simply, the relevant component can be divided into a number of segments, whose variance or energy are similar except for the segments containing abrupt changes. For example, the components in Fig. 2 can be divided into 10 blocks. For ECG or continuous noise, the variance difference between each of these segments is negligible. However, it is comparatively larger for the component containing the abrupt changes, and this can be used to identify that component.

In our approach, a 10-second epoch of ECG is firstly chosen for ICA processing. Next, the Kurtosis value of each ICA component is calculated. A component whose modulus of Kurtosis is below the threshold is marked as continuous noise. Then, the

remaining ICA components are divided into 10 non-overlapping blocks, each of one-second duration. The variances of the 10 segments for each component are calculated as shown in Eq. (8), then the variance of these ten variance values is obtained as the parameter  $Var_{var}$ . The component whose  $Var_{var}$  value is above a pre-determined threshold is marked as an abrupt change component. Finally, the corrected ECG can be obtained using equations (3) and (6).

## 2.3 Materials

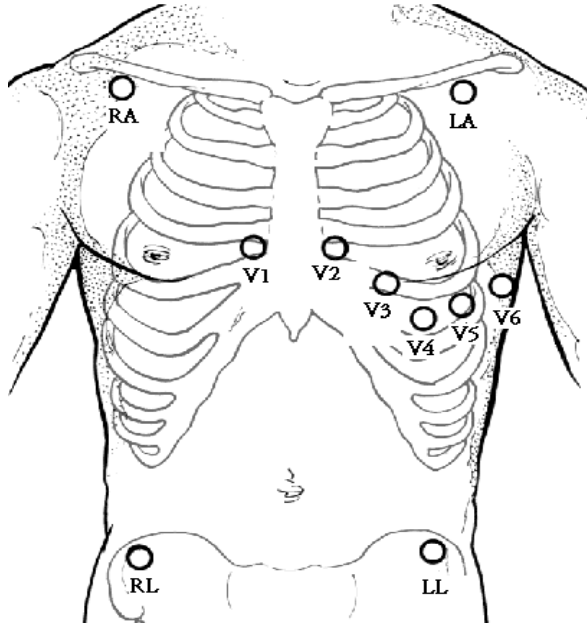


**Fig.3.** Standard electrode points for clinical ECG monitoring.

The data analysed were collected from patients at the John Radcliffe Hospital in Oxford using a multi-parameter patient monitoring system [20]. The patients were drawn from a variety of wards (but principally from the Coronary Care Unit) and had different medical conditions. The cardiac signals were measured using a set of electrodes conforming to the standard ECG electrode placement points (Fig.3). Only three electrodes are used, one at V5, one at RA (Right Arm) and one at LL (Left Leg). They correspond to two different clinical channels, V5 and lead II, as well as a third channel with no specifically defined meaning [21]. In order to keep the number of electrodes on the patient to a minimum, there is no reference electrode and so the ground is taken to be the average of the three different channels.

The ECG is sampled at 256Hz, in line with the 1994 ANSI standards [22]. An FIR band-pass filter (Table 1) is designed using the Parks-McClellan algorithm [23, 24]. Filters designed by this method exhibit an equi-ripple behaviour in their frequency response, and have a linear phase response over the range of interest, so that the shape of the ECG waveform is not distorted.

The data were not pre-selected with respect to quality, and recordings lasting over several hours from 10 patients were used for the analysis described in this paper.

**Table 1.** Filter Properties used for coefficient generation with Matlab 5

Filter Type	f1 (Hz)	f2 (Hz)	Rs (dB)	Rp (dB)	fs (Hz)	Order
High Pass	0.00128	1.28	48	2.096	256	312
Low Pass	35	45	48.25	1.925	256	37

In Table 1, Rs is the minimum attenuation in the stop band. The transition band lies between frequencies f1 and f2. Rp is the ripple in the pass band, fs is the sampling frequency and the order is the number of coefficients required to meet the attenuation criterion.

### 3. Choice of thresholds for detection of continuous noise and abrupt changes

Three-channel ECG recordings from 10 patients were used in this study. For the identification approach, the 10 data sets were divided into two groups, six of them being used to determine the thresholds needed with the other 4 set aside for evaluating the performance of the proposed technique.

100 blocks of ECG data, each with a period of 10 seconds, were extracted from the first six data sets. The data were processed using the ICA algorithm described above, then the  $|Kurt|$  and  $Var_{var}$  values were calculated in each case. From the analysis of the results, the thresholds were set to 5 for the value of  $|Kurt|$ , and 0.5 for the value of  $Var_{var}$ , i.e. a component for which the modulus of  $Kurt$  is less than 5 will be considered to be continuous noise and a component whose  $Var_{var}$  value is greater than 0.5 will be marked as corresponding to an abrupt change.

A further 60 blocks of ECG data, each with a period of 10 seconds, were extracted from the remaining 4 validation data sets. This showed that all the noise and abrupt changes were correctly identified using the chosen thresholds.

## 4. Results

**Example 1: Noise in one channel (subject 2, time period: 80s–90s)**

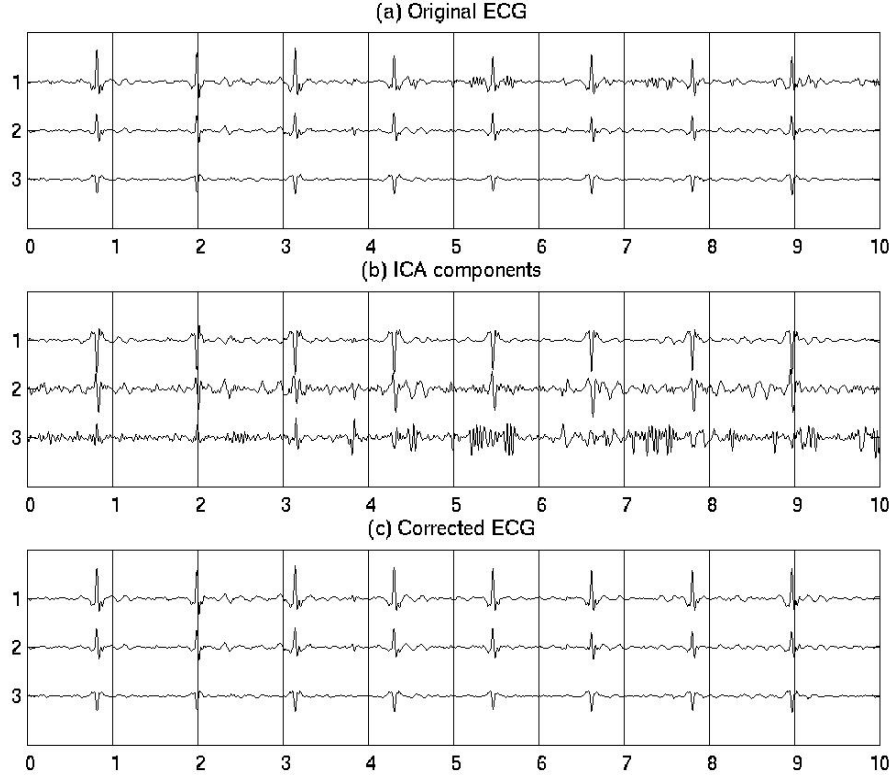


**Fig. 4.** Demonstration of ECG artefact removal by ICA (a) 10s of ECG data, with channel 1 contaminated with noise. (b) Corresponding ICA components. (c) Corrected ECG signals by removing the third component in (b).

**Table 2.** The Values of  $|Kurt|$  and  $Var_{var}$  for each of the 3 ICA components

Index	ICA1	ICA2	ICA3
$ Kurt $	24.09	6.97	<b>2.84</b>
$Var_{var}$	0.17	0.2	0.42

Fig. 4(a) shows a 10s portion of ECG data. It can be clearly seen that channel 1 is contaminated with noise, seen as abnormal oscillations either side of the 5<sup>th</sup>, 7<sup>th</sup> and 8<sup>th</sup> QRS complexes. Fig. 4(b) shows the corresponding components derived by ICA. The noise in the original ECG is separated as ICA component 3, whose  $|Kurt|$  value is 2.84 (Table. 2). Fig. 4(c) shows the ‘corrected’ ECG when the noise component is removed by setting the third row of the  $V$  matrix to zero (c.f. Eq. (6)).

In this case, the noise source can be effectively identified and removed from the original signal.

**Example 2: Noise in two channels (subject 1, time period: 1200s–1210s)**

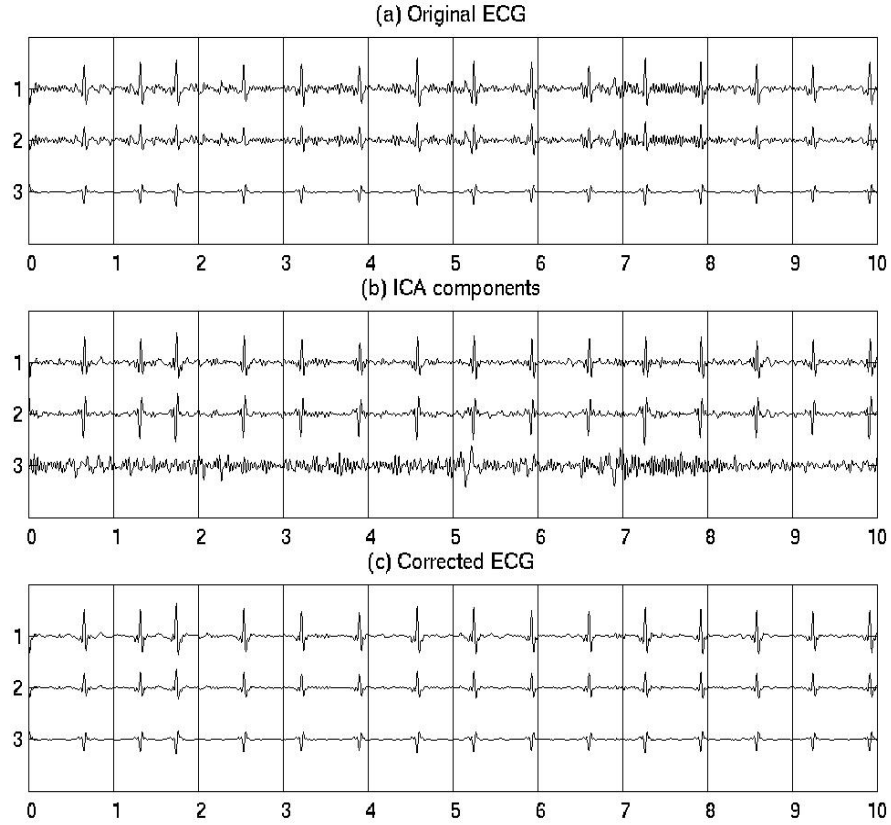


**Fig. 5.** Demonstration of ECG artefact removal by ICA (a) 10s of EEG data, with channels 1 and 2 contaminated with noise. (b) Corresponding ICA components. (c) Corrected ECG signals by removing the third component in (b).

**Table 3.** The Values of  $|Kurt|$  and  $Var_{var}$  for each of the 3 ICA components

Index	ICA1	ICA2	ICA3
$ Kurt $	12.89	13.37	<b><u>1.61</u></b>
$Var_{var}$	0.1	0.12	0.2

Fig. 5(a) shows a 10s portion of ECG data. It can be clearly seen that both channel 1 and channel 2 are contaminated with noise. Fig. 5(b) shows the corresponding components derived by ICA. The noise in the original ECG is separated as ICA component 3, whose  $|Kurt|$  value is 1.61 (Table 3). Fig. 5(c) shows the ‘corrected’ ECG by removing the noise component of ICA, again the third component in Fig. 5(b).

In this case, the noise source is also clearly identifiable and it can be removed from the original signal. Note also that the third QRS complex is of abnormal shape and timing. This is possibly an ectopic beat [25], not identified as artefact or noise by the ICA algorithm, and is consequently not removed.

**Example 3: Artefacts in one channel (subject 3, time period: 240s–250s)**

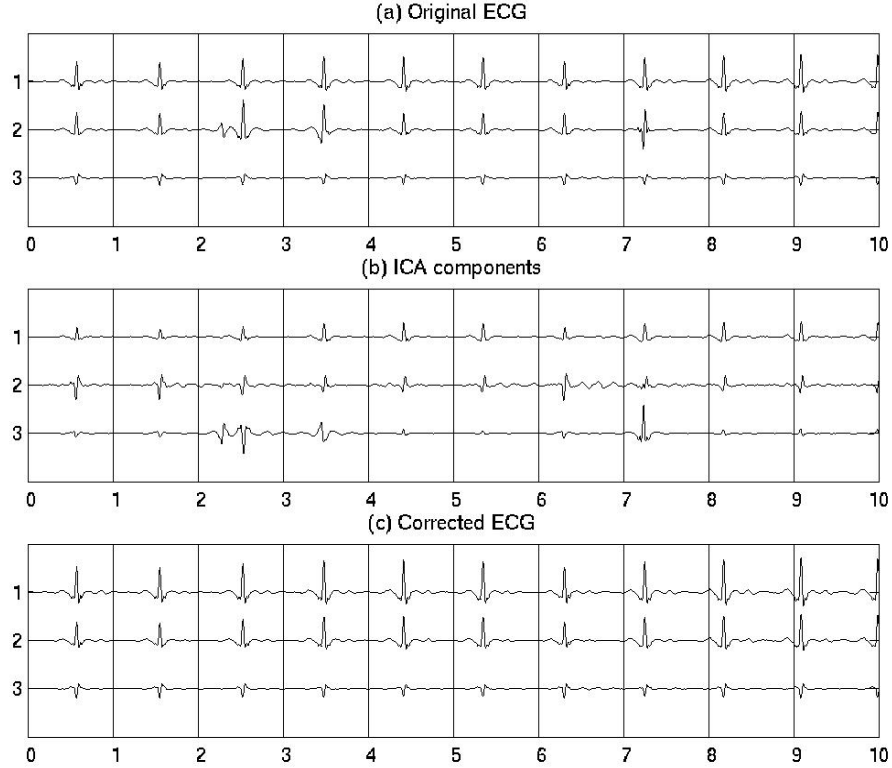


**Fig. 6.** Demonstration of ECG artefact removal by ICA (a) 10s of ECG data, with artefacts in channel 2 (2–3s and 7–8s). (b) Corresponding ICA components. (c) Corrected ECG signals by removing the third component in (b).

**Table 4.** The Values of  $|Kurt|$  and  $Var_{var}$  for each of the 3 ICA components

Index	ICA1	ICA2	ICA3
$ Kurt $	20	115.24	56.33
$Var_{var}$	0.35	0.25	<b><u>2.44</u></b>

Fig. 6(a) shows a 10s portion of ECG data. It can be seen that there are two artefacts in channel 2, during the periods from 2 to 3s, 3 to 4s and 7 to 8s. Fig. 6(b) shows the corresponding components derived by ICA. The artefacts in the original ECG are again isolated to ICA component 3 with the  $Var_{var}$  value being 2.44 (Table 4). Fig. 6(c) shows the ‘corrected’ ECG by removing the artefact component of ICA, setting it to zero as before.

Although the artefacts occur at the same time as the QRS complexes in this case, they can still be removed from the relevant QRS complexes. Furthermore, the second artefact (within the period 3–4s) is obvious in ICA component 3, though it could easily have been ignored in the original signals.

**Example 4: Noise plus artefact in two channels (subject 1, time period:1010s–1020s)**

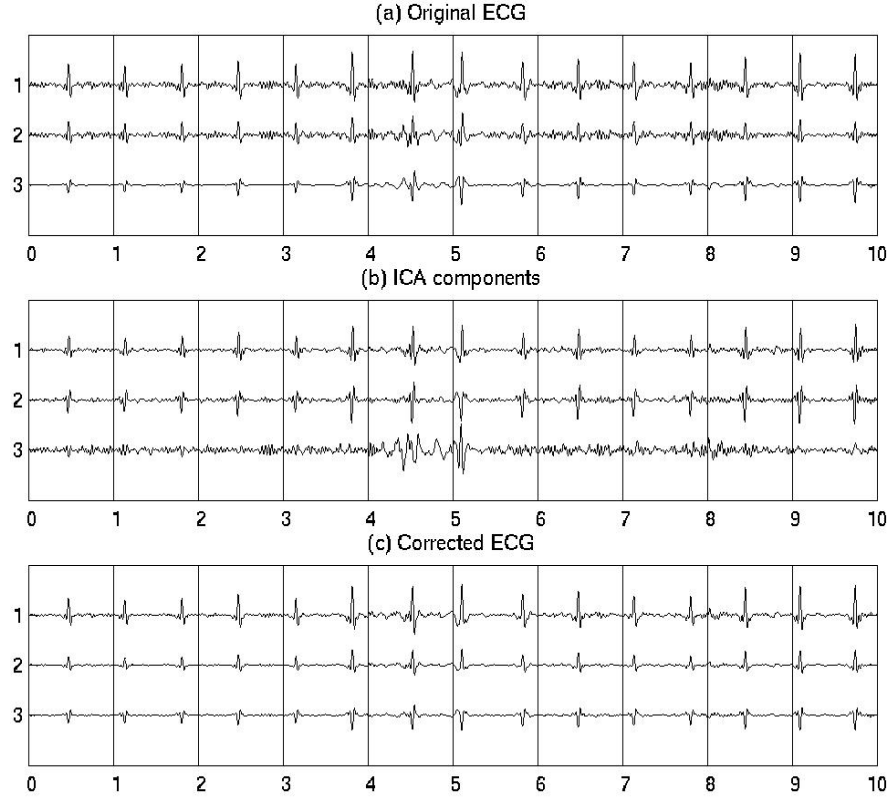


**Fig. 7.** Demonstration of ECG artefact removal by ICA (a) 10s of ECG data, with artefacts in channels 2 and 3 (4–6s), noise in channels 1&2. (b) Corresponding ICA components. (c) Corrected ECG signals by removing the third component in (b).

**Table 5.** The Values of  $|Kurt|$  and  $Var_{var}$  for each of the 3 ICA components

Index	ICA1	ICA2	ICA3
$ Kurt $	16.54	14.97	8.95
$Var_{var}$	0.25	0.21	<u>1.22</u>

Fig. 7(a) shows a 10s portion of ECG data. It can be clearly seen that there are artefacts in channels 2 and 3, within the period from 4 to 6s (note also the distorted QRS complexes caused by the artefacts) and noise in channels 1 and 2. Fig. 7(b) shows the corresponding components derived by ICA. As before the artefacts and noise in the original ECG are isolated to ICA component 3, the  $Var_{var}$  value being 1.22 (Table 5). Fig. 7(c) shows the ‘corrected’ ECG by removing the artefacts and noise component of ICA.

In this case, when the artefacts and ectopic beats are coincident, the former can be effectively detected and removed from the original signal.

**Example 5: Artefacts in 3 channels (Subject 1, time period: 840–850)**

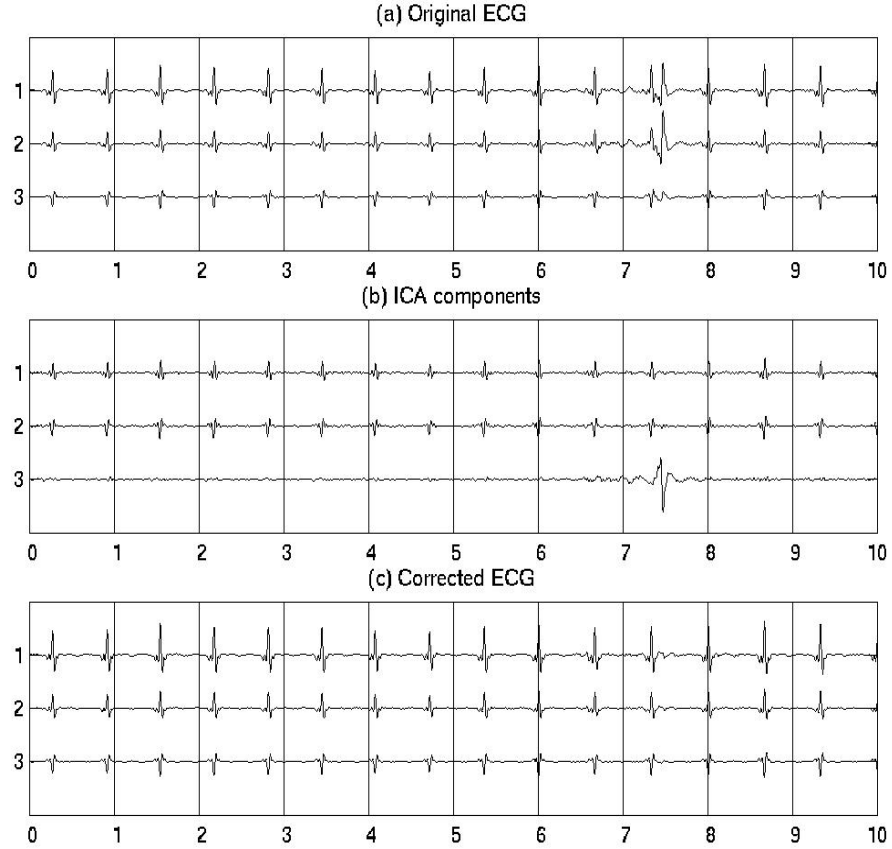


**Fig. 8.** Demonstration of ECG artefact removal by ICA (a) 10s of ECG data, with artefacts in all 3 channels (7s–8s), (b) Corresponding ICA components. (c) Corrected ECG signals by removing the third component in (b).

**Table 6.** The Values of  $|Kurt|$  and  $Var_{var}$  for each of the 3 ICA components

Index	ICA1	ICA2	ICA3
$ Kurt $	14.71	14.44	104.74
$Var_{var}$	0.11	0.06	<b>8.01</b>

Fig. 8(a) shows a 10s portion of ECG data. It can be clearly seen that there is an artefact just after 7s which affects all 3 channels. Fig. 8(b) shows the corresponding components derived by ICA. The artefacts are also isolated to ICA component 3, the  $Var_{var}$  value being 8.01 (Table 6). Fig. 8(c) shows the ‘corrected’ ECG by removing the artefacts component of ICA.

In the case of an artefact affecting all 3 channels at the same time, it can be effectively detected and removed from the original signal.

**Example 6: Noise in 3 channels (subject 2, time period: 900s–910s)**

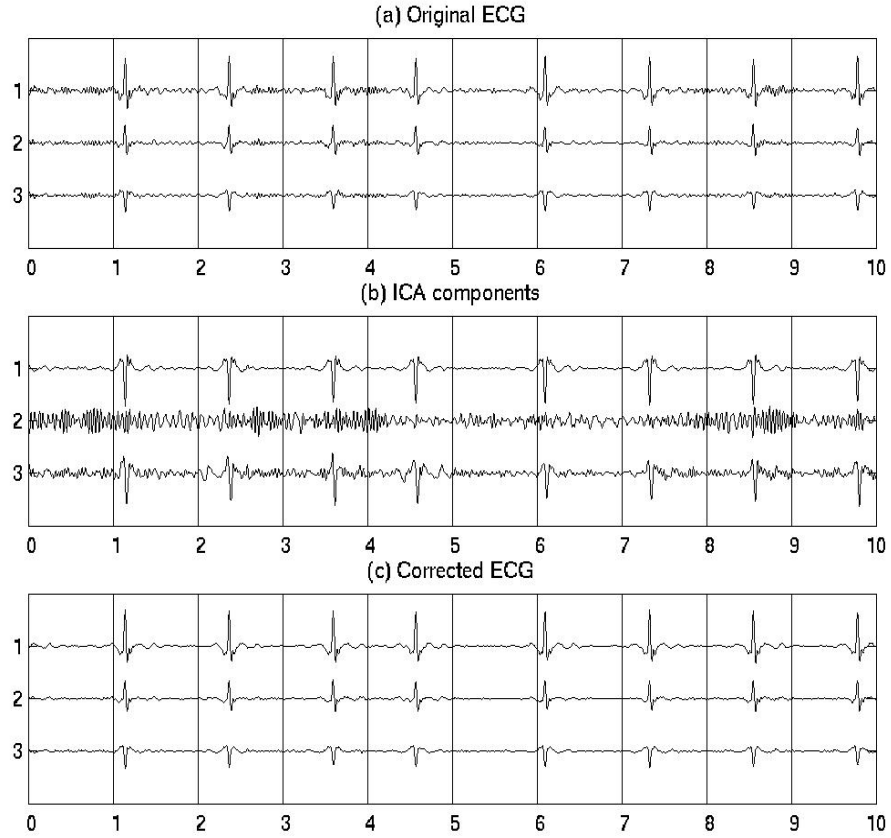


**Fig. 9.** Demonstration of ECG artefact removal by ICA (a) 10s of EEG data, with noise in all the 3 channels. (b) Corresponding ICA components. (c) Corrected ECG signals by removing the third component in (b).

**Table 7.** The Values of  $|Kurt|$  and  $Var_{var}$  for each of the 3 ICA components

Index	ICA1	ICA2	ICA3
$ Kurt $	25.92	<b>0.17</b>	12.81
$Var_{var}$	0.26	0.24	0.22

Fig. 9(a) shows a 10s portion of ECG data. It can be clearly seen that there is some high-frequency noise in all 3 channels, lasting the whole segment. Fig. 9(b) shows the corresponding components derived by ICA. The high-frequency noise is mostly isolated to ICA component 2, the  $|Kurt|$  value being 0.17 (Table 7). Fig. 9(c) shows the ‘corrected’ ECG by removing this artefactual component of ICA.

In this case, the high-frequency noise which is present in all 3 channels and lasts for the whole segment, can be effectively detected and substantially removed from the original signal.

**Example 7: Noise and artefacts in 3 channels (subject 10, time period: 359s–369s)**

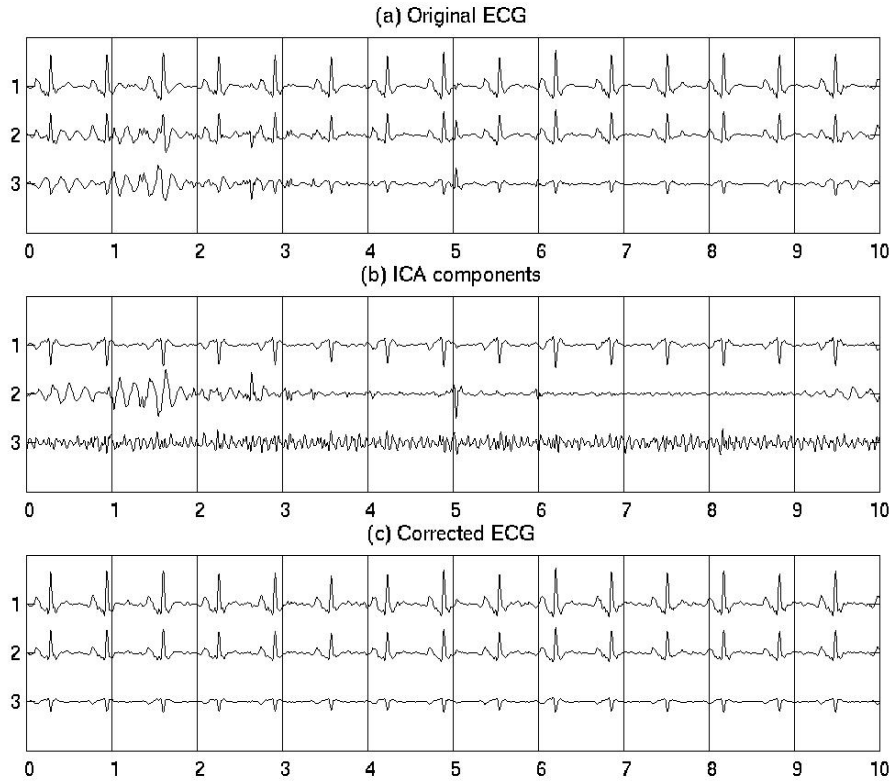


**Fig. 10.** Demonstration of ECG artefact removal by ICA (a) 10s of ECG data, with noise and artefacts in all 3 channels (0s–2s), (b) Corresponding ICA components. (c) Corrected ECG signals by removing the second and third components in (b).

**Table 8.** The Values of  $|Kurt|$  and  $Var_{var}$  for each of the 3 ICA components

Index	ICA1	ICA2	ICA3
$ Kurt $	9.52	8.46	<b><u>0.32</u></b>
$Var_{var}$	0.14	<b><u>2.94</u></b>	0.02

Fig. 10(a) shows a 10s portion of ECG data. It can be clearly seen that there is some kind of artefact and noise in all 3 channels around the period from 0 to 2s. Fig. 10(b) shows the corresponding components derived by ICA. It is also clear that the second component contain transient artefacts ( $Var_{var} = 2.94$ , Table 8) and that the third component corresponds to high frequency noise ( $|Kurt| = 0.32$ , Table 8). Fig. 10(c) shows the ‘corrected’ ECG by removing components 2 and 3 of ICA as shown in Fig. 10(b).

In this case, the artefacts and continuous noise which are present in all 3 channels can be separated into 2 different channels and removed.

**Example 8: Artefacts and Noise in 3 channels (subject 1, time period: 1210s–1220s)**

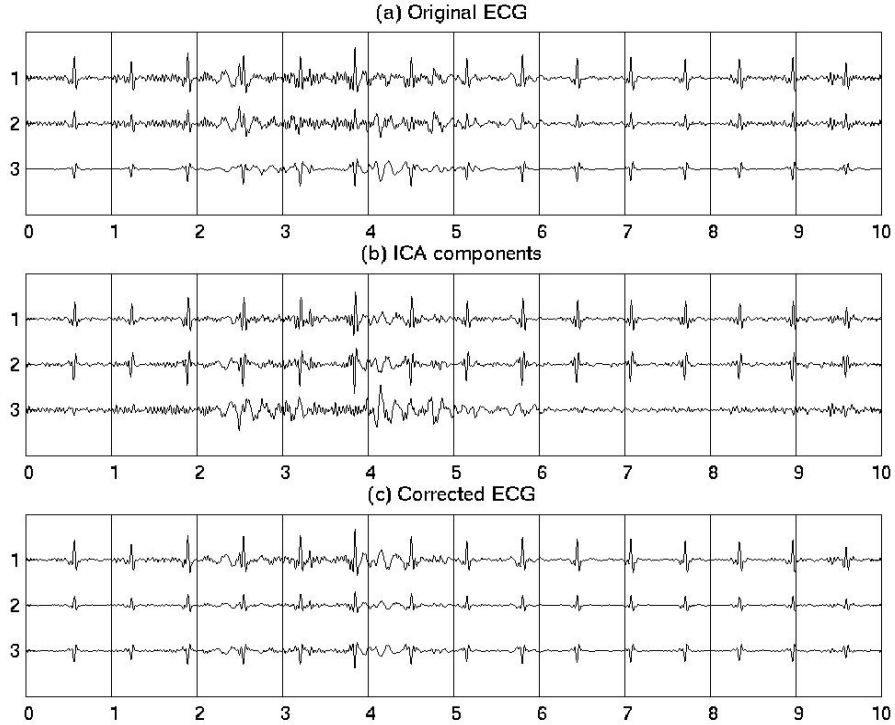


**Fig. 11.** Demonstration of ECG artefact removal by ICA (a) 10s of ECG data, with artefacts and noise in all the 3 channels. (b) Corresponding ICA components. (c) Corrected ECG signals by removing the third component in (b).

**Table 9.** The Values of  $|Kurt|$  and  $Var_{var}$  for each of the 3 ICA components

Index	ICA1	ICA2	ICA3
$ Kurt $	12.3	12.02	6.53
$Var_{var}$	0.27	0.3	<b>1.88</b>

Fig. 11(a) shows a 10s portion of ECG data. It can be clearly seen that there are artefacts and noise in all 3 channels. Fig. 11(b) shows the corresponding components derived by ICA. It is obvious that all three ICA components contain some noise and artefacts, although component 3 is the one identified as artefact ( $Var_{var} = 1.88$ , Table 9). Fig. 10(c) shows the ‘corrected’ ECG by removing artefact component 3 of ICA as shown in Fig. 11(b). Nevertheless, there still exists a lot of noise in the corrected ECG, which also includes most of the artefactual data. Therefore, ICA is not successful in removing noise or artefacts in this case.

Compared with examples 6 and 7, it seems that the artefacts are of higher amplitude leading to a low signal-to-noise ratio, which is probably the main reason why ICA fails here.

## 4. Discussion and conclusion

ICA is successful in separating artefacts and noise from the ECG using the approach detailed in this report. ICA can effectively detect and remove a considerable amount of the noise and artefacts, particularly when only one or two channels of ECGs are corrupted. This suggests that artefacts and noise are independent sources from the physiological sources generating the cardiac signals.

A limitation of ICA is that one has to rely on visual inspection of the ICA components for further processing. We have introduced a new approach to solving the above problem for the case of clinical ECG analysis. The proposed technique is based on simple statistical indices and it has been successfully tested on real ECG data. The advantage of this method is its simplicity, efficiency, and hence potential for online processing of the ECG using ICA.

ICA makes no assumption regarding the model that best describes the data. This can be viewed as advantageous, as it makes ICA general in its application. However it is also a weakness in some instances, for it does not allow inclusion of prior information concerning the signal being analysed. The ECG is a quasi periodic signal which has a distinct morphology. It should be possible to combine this prior information with current ICA algorithms and improve the rejection of artefacts from heavily corrupted signals such as those of Fig. 11.

**Acknowledgements.** Dr. Taigang He was supported by an EPSRC post-doctoral Research Assistantship (GR/M05614) and Gari Clifford was funded by Oxford BioSignals Ltd.

## References

1. Paul JS, Reddy MR, Kumar VJ. A transform domain SVD filter for suppression of muscle noise artefacts in exercise ECG's. *IEEE Trans. Biomed. Eng.* 2000; 3:654–663
2. Talmon TL, Kors JA, Von JH. Adaptive Gaussian filtering in routine ECG/VCG analysis. *IEEE Trans. Acoust., Speech, Signal Processing* 1986; ASSP-34: 527–534
3. Thakor NV, Zhu VS. Application of adaptive filtering to ECG analysis: Noise cancellation and arrhythmia detection. *IEEE Trans. Biomed. Eng.* 1991; 38:785–793
4. Bensadoun Y, Novakov E, Raoof K. Multidimensional adaptive method for canceling EMG signals from the ECG signal. In: Roberge FA, Kearney RE, editors. 17th IEEE Ann Int Conf on Engng in Med and Biol Soc. Montreal 1995, pp 299–300
5. Barros AK, Ohnishi N. MSE behavior of biomedical event-related filters. *IEEE Trans. Biomed. Eng.* 1997; 44:848–855
6. Laguna P, Janè R, Meste O, et al. Adaptive filter for event-related bioelectric signals using an impulse correlated reference input: Comparison with signal averaging techniques, *IEEE Trans. Biomed. Eng.* 1992; 39:1032–1043

7. Vaz C, Kong X, Thakor NV. An adaptive estimation of periodic signals using a Fourier linear combiner. *IEEE Trans. Signal Process.* 1994; 42:1–10
8. Kanjilal PP, Palit S. On multiple pattern extraction using singular value decomposition, *IEEE Trans. Signal Proc.* 1995; 43:1536–1540
9. Wisbeck JO, Garcia RO. Application of Neural Networks to Separate Interferences and ECG Signals. Proceedings of IEEE International Caracas Conference on Devices, Circuits and Systems, 1998, pp 291–294
10. Speirs CA, Soraghan JJ, Stewart RW, et al. Ventricular late potential detection from bispectral analysis of ST-segments. Proceedings of EUSIPCO—94, September 1994, pp 1129–1132
11. Jung T-P, Makeig S, Lee T-W, et al. The 2nd Int'l Workshop on Independent Component Analysis and Signal Separation, 2000, pp 633–44
12. Cardoso JF. Multidimensional independent component analysis. *Proc. ICASSP '98*. Seattle, 1998, pp 1941–1944
13. Wisbeck JO, Barros AK, Ojeda R. Application of ICA in the Separation of Breathing artefacts in ECG Signals. International Conference on Neural Information Processing, (ICONIP'98), Kyushu, Japan, 1998
14. Barros AK, Mansour A, Ohnishi N. Removing artefacts from electrocardiographic signals using independent component analysis. *Neurocomputing* 1998; 22:173–186
15. Tong S, Bezerianos A, Paul J, et al. Removal of ECG interference from the EEG recordings in small animals using independent component analysis, *Journal of Neuroscience Methods* 2001; 108:11–17
16. Jung TP, Makeig S, Humphries C, et al. Removing electroencephalographic artefacts by blind source separation, *Psychophysiology* 2000; 37: 163–78
17. Hyvärinen A. Survey on Independent Component Analysis. *Neural Computing Surveys* 1999; 2:94–128
18. Cardoso JF. High-order contrasts for independent component analysis. *Neural Computation* 1999; 11:157–192
19. Huber PJ. Projection pursuit. *The Annals of Statistics* 1985; 13(2):435–475, 1985.
20. Tarassenko L, Townsend N, Clifford G, et al. Medical signal processing using the Software Monitor. *Proc. of IEE/DERA workshop on Intelligent Signal Processing*, Birmingham, February 2001, pp 3/1–3/4
21. Anderson ST, WG Downs, Lander P, et al. Advanced electrocardiography. Spacelabs medical biophysical measurement, SpaceLabs Medical Inc., Washington USA, 1995
22. ANSI/AAMI EC38–1994, Ambulatory electrocardiographs. American National Standard, August 1994
23. McClellan P. Algorithm 5.1. Programs for Digital Signal Processing. IEEE Press. New York: John Wiley & Sons, 1979
24. Clifford G. The Software Monitor Project – Novelty detection and classification in Electrocardiograms. DPhil transfer report, Department of Engineering Science, University of Oxford, November 1999
25. Houghton A, Gray D. Making sense of the ECG. Oxford University Press, 1997